Anisotropic RKKY interaction in spin-polarized graphene

F. Parhizgar,[1] Reza Asgari,[1,*] Saeed H. Abedinpour,[2] and M. Zareyan[2]

[1]*School of Physics, Institute for Research in Fundamental Sciences (IPM), Tehran 19395-5531, Iran*

[2]*Department of Physics, Institute for Advanced Studies in Basic Sciences (IASBS), Zanjan 45137-66731, Iran*

We study the Ruderman-Kittel-Kasuya-Yosida (RKKY) interaction in the presence of spin polarized two-dimensional Dirac fermions. We show that an externally applied spin polarization along the z axis mediates an anisotropic interaction which corresponds to an XXZ model interaction between two magnetic moments. For undoped graphene, while the x part of interaction keeps its constant ferromagnetic sign, its z part oscillates with the distance R of magnetic impurities. A finite doping causes both parts of the interaction to oscillate with R. We explore a beating pattern of oscillations of the RKKY interaction along armchair and zigzag lattice directions, which occurs for some certain values of the chemical potential. The two characteristic periods of the beating are determined by inverse of the difference and the sum of the chemical potential and the spin polarization.

I. INTRODUCTION

The charge and spin oscillatory interactions in metals has attracted considerable attention both on theoretical and experimental sides.[1,2] Ruderman and Kittel[3] suggested that the spin oscillatory interaction in metals could provide a long-range interaction between nuclear spins in metals. Afterwards, Kasuya and Yosida[4] extended the theory to include the long-range interaction between magnetic impurities and thus the combined refers to RKKY interaction.

The recent discovery of graphene,[5] the two-dimensional crystal of carbon atoms, has provided a new material with a peculiar structure for charge and spin interactions. This stable crystal has already attracted considerable attention because of its unusual effective many-body properties[6–13] that follow from the chiral nature of linearly dispersing low-energy excitations described by pair of Dirac cones at the K and K' edges of the first Brillouin zone.

The RKKY interaction in pristine graphene has been studied by several groups.[14–16] Due to the particle-hole symmetry of graphene, the RKKY interaction induces ferromagnetic correlations between magnetic impurities on the same sublattice, and antiferromagnetic correlations between those on different sublattices. The dependence of the interaction on the distance R between two local magnetic moments, at the Dirac point, is found to be R^{-3}, whereas it behaves as R^{-2} in conventional two-dimensional (2D) systems.[17] Such a fast decay rate means that the interaction is rather short ranged. In doped graphene, on the other hand, the spatial dependence of the interaction is predicted to be similar to conventional 2D systems, but this still remains to be experimentally verified.

Due to the fact that the RKKY interaction is originated by the exchange coupling between the impurity moments and the spin of itinerant electrons in the bulk of the system, spin polarization of electrons is expected to influence directly this interaction.[18] In particular, the combination of the spin dependence with a Dirac-like spectrum can mediate a much richer collective behavior of magnetic adatoms.[19] This has been explained for surface states of a three-dimensional topological insulator, on which magnetic impurities exhibit a frustrated RKKY interaction with two possible phases:

an ordered ferromagnetic phase and a disordered spin-glass phase.[20] Graphene, in particular, with imbalanced chemical potentials of spin-up and spin-down electrons, presents a unique spin chiral material in which the interplay between the spin polarization, gapless spectrum, and the chiral nature of electrons has been shown to result in intriguing phenomena.[21] In the two-dimension graphene system, the polarization of the chemical potential can be tuned to be of order or even higher than the mean chemical potential; a condition which is not possible in ordinary conductors. The aim of the present study is to address the question of how this peculiarity can affect the collective coupling of magnetic impurities on the surface of a graphene sheet with a finite polarization of the spin. One would expect that the interplay or interference between an externally applied polarization of the spin and the spin density wave produced by magnetic ad atoms on a graphene sheet leads to novel collective phenomena.

In this work, we calculate the RKKY interaction mediated by spin-polarized Dirac fermions in monolayer graphene using the Green's function method. Our theory for the spin-polarization dependence of the RKKY interaction is motivated not only by fundamental transport considerations, but also by application and potential future experiments in the field of graphene spintronics. With a spin polarization along the z axis, we show that the RKKY interaction is anisotropic, corresponding to an XXZ-model interaction between the two magnetic moments when their spin orientations are fixed. This Hamiltonian can be used to investigate the ground-state phase diagram of magnetic ordering of randomly distributed adatoms on the surface of spin-polarized graphene in the dilute limit.[22] Such a study has been of great interest because it provides an important contribution to the physics of magnetic graphene in particular and to spintronic technological applications in general. Besides the R^{-3} dependence of the interaction for undoped graphene, we show in particular that the interaction behaves like R^{-2} when the spin polarization is finite. In addition, a beating pattern for the interaction in the cases where impurities are located along certain directions is obtained near the resonance condition which is controlled by the chemical potential and the spin polarization.

The paper is organized as follows: In Sec. II we introduce the formalism that will be used in calculating the RKKY interaction from the lattice Green's function. In Sec. III we present our analytic and numeric results for the coupling strengths of the RKKY interaction in both undoped and doped graphene sheets. Section IV contains discussions and a brief summary of our main results.

II. METHOD AND THEORY

We consider a spin-polarized graphene system identified by a spin-dependent chemical potential μ_s ($s = \pm 1$), implying a mean chemical potential $\mu = \sum_s \mu_s/2$ and the spin polarization $\mu_p = \sum_s s\mu_s/2$. Such a spin polarization can be injected, for instance, by ferromagnetic electrodes on top of the graphene sheet.[23,24] Intrinsic ferromagnetic correlations are also predicted to exist in graphene sheets[25] and nanoribbons with zigzag edges[26] under certain conditions.

The electronic structure of spin-polarized graphene can be reasonably well described using a rather simple tight-binding Hamiltonian, leading to analytical solutions for their energy dispersion and related eigenstates. The noninteracting nearest-neighbor tight-binding Hamiltonian for π-band electrons with spin s is determined by[27]

$$\hat{\mathcal{H}}_0^s = -t \sum_{\langle i,j \rangle}(a_{i,s}^\dagger b_{j,s} + b_{i,s}^\dagger a_{j,s}) - s\mu_p \sum_i (a_{i,s}^\dagger a_{i,s} + b_{i,s}^\dagger b_{i,s}),$$
$$(1)$$

where $a_{i,s}$ ($b_{i,s}$) annihilates an electron with spin s on sublattice A (B) of unit cell i and $t \simeq 2.9$ eV denotes the nearest-neighbor hopping parameter.[28] The sum $\langle i,j \rangle$ in Eq. (1) runs over distinct nearest neighbors.

The s component of the noninteracting Hamiltonian in momentum space is written as

$$\hat{\mathcal{H}}_0^s = \begin{pmatrix} -s\mu_p & f(\mathbf{k}) \\ f^*(\mathbf{k}) & -s\mu_p \end{pmatrix}, \qquad (2)$$

where the form factor in the general case is $f(\mathbf{k}) = -t \sum_j e^{i\mathbf{k}\cdot\mathbf{d}_j}$, in which $\mathbf{d}_j$s are nearest-neighbor position vectors. In this work, we are interested in the low-energy behavior, in which $f(\mathbf{k}) = v_F k \Phi(k)$, where $\Phi(k) = e^{i(\pi/3+\theta_k)}$ at the Dirac point K and $\Phi(k) = -e^{i(\pi/3-\theta_k)}$ at the other Dirac point K', the chiral angle is $\theta_k = \tan^{-1}(k_x/k_y)$, $v_F = 3ta/(2\hbar) \simeq 10^6$ m/s is the Fermi velocity with $a \simeq 1.42$ Å being the carbon-carbon distance in the honeycomb lattice.

Our system incorporates two localized magnetic moments whose interaction is mediated through a spin-polarized electron liquid. We assume that the graphene is spin polarized first, and then we add the magnetic moments. There are number of ways in experiments that a spin-polarized graphene can be made. Spin-polarized electron emission from the graphene/Ni system before and after exposure to oxygen has been recently studied[29] and the study of spin polarization of secondary electrons obtained from this system upon photoemission suggested the use of passivated Ni surfaces as a source of spin-polarized electrons, since it is stable against adsorption of reactive gases. Incidentally, the contact interaction between the spin of itinerant electrons and two magnetic impurities

with magnetic moments $\mathbf{M_1}$ and $\mathbf{M_2}$, located respectively at $\mathbf{R}_1$ and $\mathbf{R}_2$, is given by

$$\hat{\mathcal{H}}_{\text{int}} = \lambda \sum_{j=1,2} \mathbf{M}_j \cdot \mathbf{s}(\mathbf{R}_j), \qquad (3)$$

where λ is the coupling constant between conduction electrons and impurity, $\mathbf{s}(\mathbf{r}) = \frac{\hbar}{4}\sum_i \delta(\mathbf{r}_i - \mathbf{r})\boldsymbol{\sigma}_i$ is the spin density operator[1] with $\mathbf{r}_i$ and $\boldsymbol{\sigma}_i$ being respectively the position and vector of spin operators of the ith electron.

The RKKY interaction, which arises from quantum effects, is obtained by using a second-order perturbation[3,4,30,31] which reads as (from now on we set $\hbar = 1$)

$$\hat{\mathcal{H}}_{\text{RKKY}}^{\alpha\beta} = \frac{-\lambda^2}{\pi}\text{Im}\int_{-\infty}^{\infty}d\varepsilon\,\text{Tr}[(\mathbf{M}_1\cdot\boldsymbol{\sigma})G_{\alpha\beta}(\mathbf{R}_1,\mathbf{R}_2;\varepsilon)$$
$$\times (\mathbf{M}_2\cdot\boldsymbol{\sigma})G_{\beta\alpha}(\mathbf{R}_2,\mathbf{R}_1;\varepsilon)]n(\mu), \qquad (4)$$

where $n(\mu)$ denotes the Fermi-Dirac distribution function, $\boldsymbol{\sigma}$ is the vector of Pauli matrices in the *spin* space, $G_{\alpha\beta}(\mathbf{R}_1,\mathbf{R}_2;\varepsilon)$ is a 2×2 matrix of the single-particle retarded Green's function in spin space, α and β refer to the sublattices where two impurities are placed and, finally, the trace is taken over the spin degree of freedom.

For spin-unpolarized graphene, Eq. (4) simplifies to $\hat{\mathcal{H}}_{\text{RKKY}}^{\alpha\beta} = \frac{\lambda^2}{4}\chi(\mathbf{R}_1,\mathbf{R}_2)\mathbf{M}_1\cdot\mathbf{M}_2$, where $\chi(\mathbf{R}_1,\mathbf{R}_2)$ is the spin susceptibility of the itinerant electrons and determines the indirect interaction between two local moments.

In order to calculate the interaction Hamiltonian of Eq. (4), the form of the electronic single-particle Green's function, $G^s(\mathbf{R}_1,\underline{\mathbf{R}}_2;\varepsilon) = \langle\mathbf{R}_1|(\varepsilon + i0^+ - \hat{\mathcal{H}}_0^s)^{-1}|\mathbf{R}_2\rangle$ is needed. To calculate the retarded Green's function in real space, its Fourier components in momentum space might be first obtained. Due to the fact that our 2D Dirac fermion system is noninteracting and thus the direction of spin remains unchanged, the retarded Green's functions $G_{\alpha\beta}$ are diagonal in the spin space:

$$G_{AA}^s(\mathbf{R},0,\varepsilon) = (e^{i\mathbf{K}\cdot\mathbf{R}} + e^{i\mathbf{K}'\cdot\mathbf{R}})g_{AA}(\varepsilon - s\mu_p), \qquad (5)$$

and

$$G_{AB}^s(\mathbf{R},0,\varepsilon) = e^{i\pi/3}(e^{i\mathbf{K}\cdot\mathbf{R}+i\theta_R} - e^{i\mathbf{K}'\cdot\mathbf{R}-i\theta_R})$$
$$\times g_{AB}(\varepsilon - s\mu_p). \qquad (6)$$

Moreover, $G_{BB}^s = G_{AA}^s$ and $G_{BA}^s(0,\mathbf{R},\varepsilon) = \exp(-i\pi/3)$ $[\exp(-i\mathbf{K}\cdot\mathbf{R} - i\theta_R) - \exp(-i\mathbf{K}'\cdot\mathbf{R} + i\theta_R)]g_{AB}(\varepsilon - s\mu_p)$. Here $g_{AA}(\varepsilon) = \gamma\varepsilon K_0(-i\varepsilon R/v_F)$ and $g_{AB}(\varepsilon) = \gamma\varepsilon K_1(-i\varepsilon R/v_F)$, where $K_0(x)$ and $K_1(x)$ are modified Bessel functions of the second kind, θ_R is the angle of the position $\mathbf{R}$ with respect to the $\mathbf{K}' - \mathbf{K}$ direction, and $\gamma = -2\pi/(\Omega v_F^2)$, in which Ω is the area of the Brillouin zone.

By inserting the retarded Green's functions given by Eqs. (5) and (6) in Eq. (4), and taking the trace over the spin degree of matrices, the RKKY Hamiltonian simplifies to

$$\mathcal{H}_{\text{RKKY}}^{\alpha\beta} = \frac{\lambda^2}{\pi}\big[J_x^{\alpha\beta}(M_{1x}M_{2x} + M_{1y}M_{2y}) + J_z^{\alpha\beta}M_{1z}M_{2z}\big],$$
$$(7)$$

which is the honored XXZ model. Here $J_x^{\alpha\beta} = -C\Phi_{\alpha\beta}I_x^{\alpha\beta}/R^3$ and $J_z^{\alpha\beta} = -C\Phi_{\alpha\beta}I_z^{\alpha\beta}/R^3$, with $C =$

$2(2\pi)^2/(\Omega^2 v_{\rm F})$, $\Phi_{AA} = 1 + \cos[(\mathbf{K} - \mathbf{K}') \cdot \mathbf{R}]$, and $\Phi_{AB} = -1 + \cos[(\mathbf{K} - \mathbf{K}') \cdot \mathbf{R} + 2\theta_R]$. The different components of $I^{\alpha\beta}$ for impurities on the same sublattice read as

$$I_x^{AA} = 2\text{Im}\left[\int_{-\infty}^{y_{\rm F}} dy\, x_- K_0(-ix_-) x_+ K_0(-ix_+)\right],$$

$$I_z^{AA} = \text{Im}\left[\int_{-\infty}^{y_{\rm F}} dy \sum_{s=\pm} x_s^2 K_0^2(-ix_s)\right], \quad (8)$$

where $y_{\rm F} = \mu R/v_{\rm F}$, $x_\pm = y \pm h_{\rm F}$, $y = \varepsilon R/v_{\rm F}$, and $h_{\rm F} = \mu_p R/v_{\rm F}$. For impurities on different sublattices, one only needs to replace $K_0(x)$ with $K_1(x)$ in the above equations. Note that $J^{BB} = J^{AA}$ and $J^{BA} = J^{AB}$.

We find analytic results for the z component of the RKKY exchange coupling strength I_z for both cases where magnetic moments are located on the same or different sublattices. For the same-sublattice case, we begin by splitting the integral in the second line of Eq. (8) into the conduction- and valance-band contributions and find

$$I_z^{AA}(R) = 2\text{Im}\left[\int_{-\infty}^{0} dx\, x^2 K_0^2(-ix)\right]$$
$$+ \sum_{s=\pm} \text{Im}\left[\int_0^{x_{\rm Fs}} dx\, x^2 K_0^2(-ix)\right], \quad (9)$$

where $x_{F\pm} = y_{\rm F} \pm h_{\rm F}$. The first integral can be solved[15,16] easily and the result is $\pi^2/32$. The contribution from the second line of Eq. (9) can be obtained by replacing $\text{Im}[K_0^2(-ix)]$ with $-\pi^2\text{sgn}(x)J_0(|x|)Y_0(|x|)/2$ and using the following relation:

$$\int_0^{x_{\rm F}} dx\, x^2 \text{sgn}(x) J_0(|x|) Y_0(|x|) = -\frac{|x_{\rm F}|}{2\sqrt{\pi}} M(x_{\rm F}), \quad (10)$$

where $M(x) = G[\{\{\frac{1}{2}\}, \{\frac{3}{2}\}\}, \{\{1,1\}, \{-\frac{1}{2},1\}\}, x^2]$ is Meijer G function.[32] As a result, the function I_z^{AA} is given by

$$I_z^{AA}(R) = \frac{\pi^2}{4} \sum_{s=\pm} \left[\frac{1}{8} + \frac{|x_{\rm Fs}|}{\sqrt{\pi}} M(x_{\rm Fs})\right]. \quad (11)$$

To calculate the long-range behavior of the RKKY interaction, the asymptotic behavior of the Meijer G function is needed. It is also easy to see that asymptotic behavior of $M(x)$ at large x is[32] $[2\cos(2x) + 8x\sin(2x) - \pi]/(8\sqrt{\pi}x)$. It should be noticed that the $M(x)$ tends to its long-range asymptotic expression for $x > 2$. Therefore, $I_z^{AA}(R)$ for the long-range regime is simplified as

$$I_z^{AA}(R \gg a) \approx \frac{\pi}{16} \sum_{s=\pm} [\cos(2x_{Fs}) + 4x_{Fs}\sin(2x_{Fs})]. \quad (12)$$

On the other hand, for the case that the impurities are located on two different sublattices we can follow the same procedure discussed above, while we use $\int_{-\infty}^{0} dx\, x^2 \text{Im}[K_1^2(-ix)] = 3\pi^2/32$, and $\text{Im}[K_1^2(-ix)] = \pi^2\text{sgn}(x)J_1(|x|)Y_1(|x|)/2$ to find

$$\int_0^{x_F} dx\, x^2 \text{sgn}(x) J_1(|x|) Y_1(|x|) = -\frac{|x_F|}{2\sqrt{\pi}} M'(x_F), \quad (13)$$

where $M'(x) = G[\{\{\frac{1}{2}\}, \{\frac{3}{2}\}\}, \{\{1,2\}, \{-\frac{1}{2},0\}\}, x^2]$. Finally, the $I_z^{AB}(R)$ reads as

$$I_z^{AB}(R) = \frac{\pi^2}{4} \sum_{s=\pm} \left[\frac{3}{8} - \frac{|x_{Fs}|}{\sqrt{\pi}} M'(x_{Fs})\right]. \quad (14)$$

The asymptotic behavior of $M'(x)$ at large x is $[3\pi - 10\cos(2x) - 8x\sin(2x)]/(8\sqrt{\pi}|x|)$. Therefore, the long-range behavior of I_z^{AB} is obtained as

$$I_z^{AB}(R \gg a) \approx \frac{\pi}{16} \sum_{s=\pm} [5\cos(2x_{Fs}) + 4x_{Fs}\sin(2x_{Fs})]. \quad (15)$$

It should be mentioned that we were not able to find simple analytic expressions for the in-plane components $I_x^{\alpha\beta}$ of the exchange coupling and in the next section we will present our numerical results for them.

III. NUMERICAL RESULTS AND DISCUSSIONS

In this section, we present our main results for the RKKY exchange coupling in the presence of spin-polarization Dirac fermions along the z axis by analyzing the above-calculated integrals of I_x and I_z. We extend the previously studied[16] results for dependencies on the distance R and lattice direction θ_R to the case of $\mu_p \neq 0$, for two different regimes of undoped ($\mu = 0$) and doped ($\mu \neq 0$) graphene.

For the I_z component of interactions, we solve the two expressions in Eqs. (11) and (14) numerically and then compare the results with asymptotic results obtained from the analytical expressions given by Eqs. (12) and (15), respectively. Generally, the results obtained from the two approaches match quite well in most of the cases, especially at long distances. The distance dependence of I_z for both AA and AB cases are illustrated in Fig. 1 for undoped graphene. For unpolarized graphene $\mu_p = 0$, $I_z^{AA} = I_x^{AA}$ is just a constant. At finite μ_p, the integral I_z has quite different behavior, exhibiting an oscillatory behavior as a function of R, with a linearly growing amplitude and a period given by $2\pi/h_F$, as can be obtain directly from Eq. (12). This behavior of I_z^{AA} results in an oscillatory J_z^{AA} with a decreasing amplitude as R^{-2}, which mimics the behavior of the RKKY coupling of unpolarized doped graphene.[16] We can understand this analogy by noting that the polarization induces spin-dependent doping of up- and down-spin Dirac bands of an undoped sample by shifting their chemical potential from the Dirac point. A comparison between R dependence of the integral I_z^{AA} and that of I_z^{AB} for various values of μ_p in Fig. 1(b) shows their difference at short distance while reaching each other as R increases. As $R \to 0$ the coupling interactions tend to their values of the unpolarized case where J^{AB} is three times larger than J^{AB}, as is discussed in Ref. 16.

From the numerical calculations of the integrals appearing in Eq. (8), we can also obtain the behavior of I_x^{AA} and I_x^{AB} for the RKKY interaction coupling of the components of the magnetic moments which are perpendicular to the spin-polarization axis. Figure 2(a) shows I_x^{AA} as a function
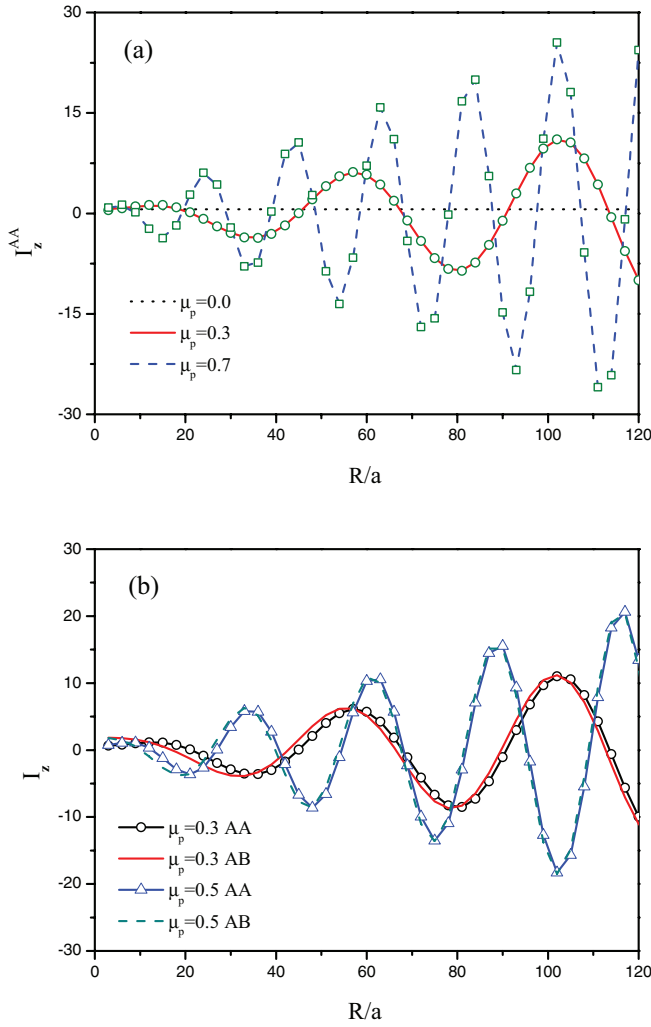
FIG. 1. (Color online) (a) Integral I_z^{AA} as a function of distance $|\mathbf{R}|$ when both impurities are located on the same sublattice for various values of the spin polarization μ_p in units of eV. The chemical potential is set to zero. Symbols refer to the analytical results of Eq. (12) which are compared to the numerical evaluation of Eq. (11), plotted as lines. For $\mu_p = 0$, $I_z^{AA} = I_z^{AB}$ is just a constant. (b) Comparison between integrals I_z^{AA} and I_z^{AB} as a function of the distance R for various values of the spin polarization μ_p in units of eV. At finite μ_p, the integral I_z has a quite different behavior, oscillating as a function of R with a period given by $2\pi/h_F$ and a linearly growing amplitude. A comparison between the R-dependence of the integral I_z^{AA} and that of I_z^{AB} shows their difference at short distance while reaching each other as R increases.
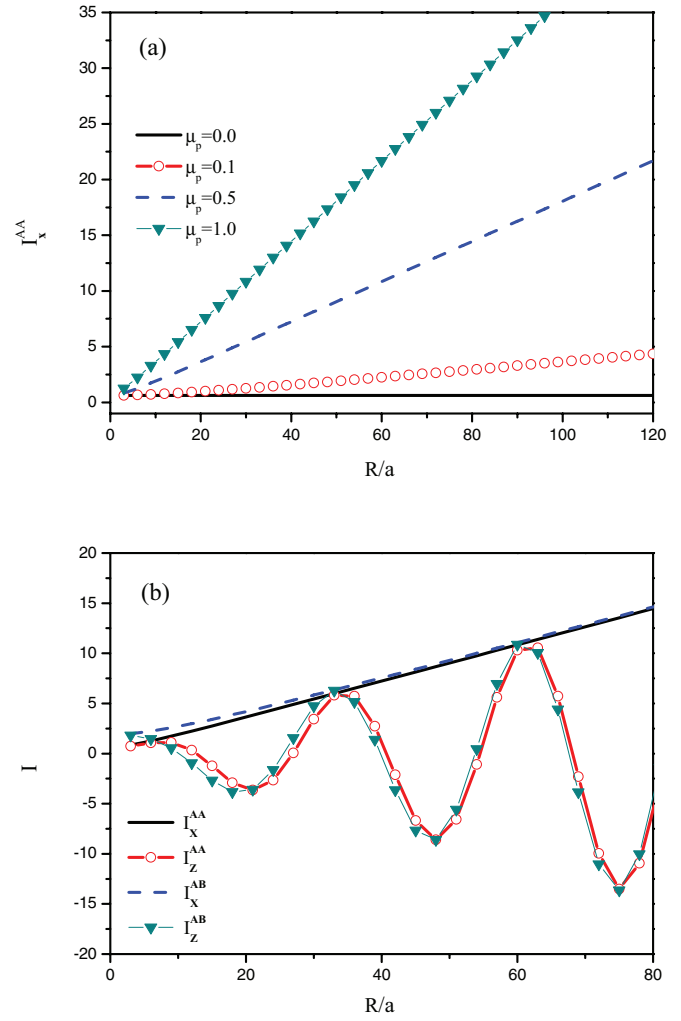
FIG. 2. (Color online) (a) Integral I_x^{AA} versus distance between two impurities, $|\mathbf{R}|$, when both impurities are located on the same sublattice for undoped graphene and for several values of μ_p in units of eV. Finite μ_p produces a linear increase of I_x^{AA} with a slope proportional to μ_p. (b) Comparison between I_x and I_z for different configurations and for $\mu_p = 0.5$ eV.

of R for the undoped graphene at different values of the spin polarization μ_p. For $\mu_p = 0$, this function is a constant resulting in a J_x^{AA} which decays as R^{-3}. A finite difference μ_p between the chemical potentials of spin-up and spin-down carriers produces a linear increase of I_x^{AA} with a slope proportional to μ_p. Thus, J_x^{AA} decays as R^{-2}. Importantly, the sign of the interaction J_x^{AA} is always positive which shows that the coupling between the perpendicular components of the moments remains ferromagnetic like for all Rs. To analyze the difference between the two configurations of AA and AB, in Fig. 2(b) we compare I_x^{AA} and I_x^{AB}, which shows that, despite

the difference at short distances, they tend to each other at larger distances.

At finite values of both the chemical potential and the spin polarization, a more complicated behavior of the RKKY coupling can be occurred. In this case, the behavior of I_z is determined by a superposition of four sinusoidal functions with two different periods of $2\pi R/(x_{F-})$ and $2\pi R/(x_{F+})$ each occurring twice with amplitudes $1, x_{F-}$ and $1, x_{F+}$, respectively. As a result, we observe that for certain values of μ and μ_p, oscillations of I_z exhibit a beating pattern with two characteristic periods. Figure 3(a) shows this beating behavior of the integral I_z^{AA} as a function of the impurity distance along the armchair direction (where $R = 3na$ with n being an integer number) for $\mu = 1.2$ eV and $\mu_p = 1.0$ eV. Figure 3(b) shows the similar behavior of the integral I_z^{AA} as a distance along the zigzag direction (where $R = \sqrt{3}ma$ for an integer m) for $\mu = 1.2\sqrt{3}$ eV and $\mu_p = \sqrt{3}$ eV. We have obtained a similar
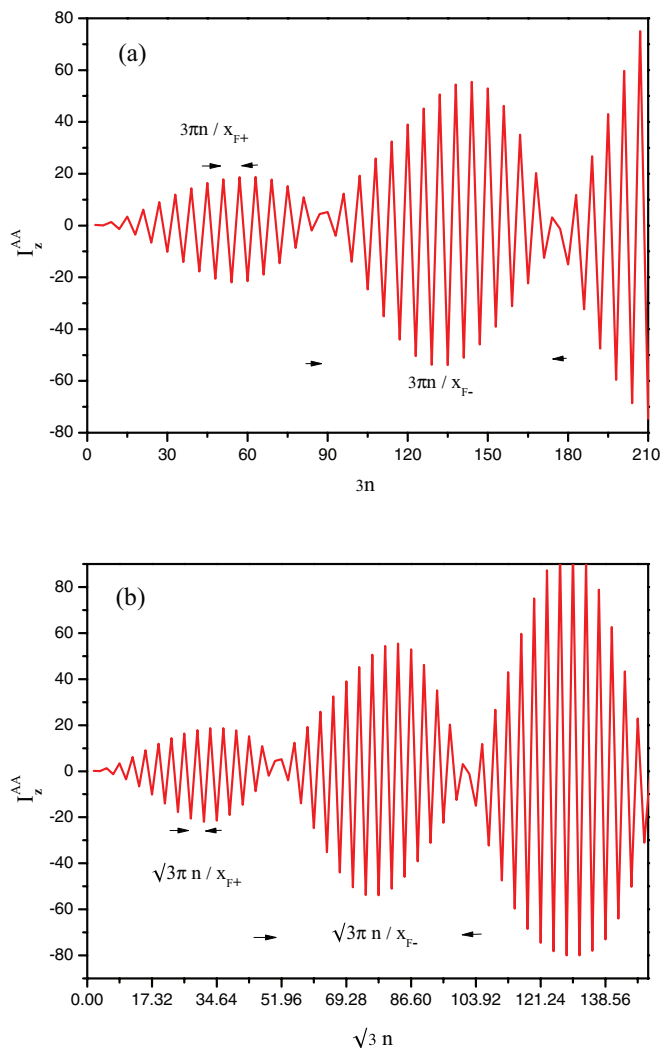
FIG. 3. (Color online) (a) Integral I_z^{AA} as a function of impurities distance along the armchair direction when both impurities are located on the same sublattice. The existence of two different periods in doped polarized graphene for certain values of $\mu = 1.2$ eV and $\mu_p = 1.0$ eV is clear in this figure. (b) Integral I_z^{AA} as a distance along zigzag direction for $\mu = 1.2\sqrt{3}$ eV and $\mu_p = \sqrt{3}$ eV.
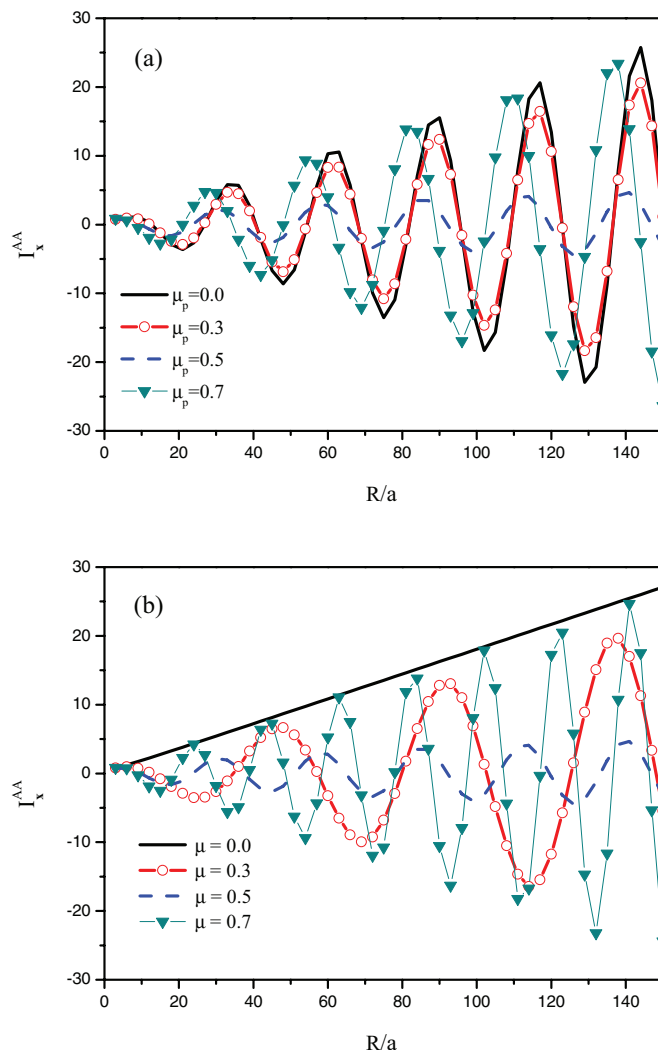

FIG. 4. (Color online) (a) Integral I_x versus distance between two impurities, $|\mathbf{R}|$, when both impurities are on the same sublattice for doped graphene with the chemical potential 0.5 eV and various value of μ_p in units of eV. (b) Same as panel (a) but for fixed $\mu_p = 0.5$ eV and various values of the chemical potential.

beating pattern for oscillations of I_z^{AB}, which also occurs for a certain values of μ and μ_p.

The behavior of the perpendicular components I_x for $\mu \neq 0$ is also different from their linear behavior for the undoped case, as shown in Fig. 4(a) for the fixed value of $\mu = 0.5$ eV and different values of μ_p. In this case $I_x(R)$ exhibits oscillations with a linearly increasing amplitude whose slope is proportional to $|\mu - \mu_p|$. Figure 4(b) is the same as Fig. 4(a), but this time μ_p is fixed and μ changes.

IV. SUMMARY AND CONCLUSIONS

In conclusion, we studied the influence of spin polarization on the RKKY interaction in graphene. With a spin polarization along the z axis, the induced interaction between two magnetic impurities is found to be described by an anisotropic XXZ Hamiltonian with an exchange coupling depending on the distance R between the impurities and the doping level. For undoped but spin-polarized graphene, we found that while the interaction between the x components of the moments remains constant with ferromagnetic sign, for the z components it oscillates with distance R. In the unpolarized-spin case, the RKKY interaction induces ferromagnetic correlations between magnetic impurities on the same sublattice and antiferromagnetic correlations between those on different sublattices.[14–16] The dependence of the interaction on the distance R between two local magnetic moments, at the Dirac point, is found to be R^{-3}, whereas it behaves as R^{-2} in a doped graphene sheet. Besides the R^{-3} dependence of the interaction for undoped graphene, we show in particular that the interaction behaves like R^{-2} when the spin polarization is finite.

For finite values of both the chemical potential and the spin polarization, a more complicated behavior of the RKKY coupling can occur. We found that both components of the interaction oscillate with R. We explored that, for the chemical

TABLE I. A breakdown of the results on the scaling form of the RKKY interactions in monolayer graphitic systems. The results for vanishing spin polarization are reported from Ref. 16 while those for finite spin polarization are from the present work. It is worthwhile mentioning that the interaction Hamiltonian is modelled by the Heisenberg model for $\mu_p = 0$ and by the XXZ model for the case that $\mu_p \neq 0$. We introduce a parameter $k_{\rm h} = \mu_p/v_{\rm F}$ and $C = (\mu - \mu_p)/(\mu + \mu_p)$ which are given by the chemical potential as well as the spin polarization.

Chemical potential	Spin polarization	Coupling of strength interaction
$\mu = 0$	$\mu_p = 0$	$J^{AA} \propto -R^{-3}$
$\mu = 0$	$\mu_p = 0$	$J^{AB} \propto R^{-3}$
$\mu \neq 0$	$\mu_p = 0$	$J^{AA} \propto -\sin(2k_{\rm F}R + \alpha)R^{-2}$
$\mu \neq 0$	$\mu_p = 0$	$J^{AB} \propto \sin(2k_{\rm F}R + \beta)R^{-2}$
$\mu = 0$	$\mu_p \neq 0$	$J_x^{AA} \propto -\mu_p R^{-2}$
$\mu = 0$	$\mu_p \neq 0$	$J_z^{AA} \propto -\sin(2k_h R)\mu_p R^{-2}$
$\mu = 0$	$\mu_p \neq 0$	$J_x^{AB} \propto \mu_p R^{-2}$
$\mu = 0$	$\mu_p \neq 0$	$J_z^{AB} \propto +\sin(2k_h R)R^{-2}$
$\mu \neq 0$	$\mu_p \neq 0$	$J_x^{AA} \propto -\sin(2k_{\rm F}R)R^{-2}$
$\mu \neq 0$	$\mu_p \neq 0$	$J_z^{AA} \propto -[\sin(2x_{\rm F+}) + C\sin(2x_{\rm F-})]R^{-2}$
$\mu \neq 0$	$\mu_p \neq 0$	$J_x^{AB} \propto \sin(2k_{\rm F}R)R^{-2}$
$\mu \neq 0$	$\mu_p \neq 0$	$J_z^{AB} \propto [\sin(2x_{\rm F+}) + C\sin(2x_{\rm F-})]R^{-2}$

potentials μ close to the polarization μ_p, oscillations of the RKKY interaction exhibit a beating pattern when the impurities are located along zigzag or armchair directions. The two characteristic periods of the beating oscillations are determined by inverse of the difference and the sum of the chemical potential and the spin polarization. Since several works on RKKY interaction in 2D graphene systems are available, a proper comparison with those results seems to be in order (see Table I).

*asgari@ipm.ir

[1] G. F. Giuliani and G. Vignale, *Quantum Theory of the Electron Liquid* (Cambridge University Press, Cambridge, 2005).

[2] M. W. Wu, J. H. Jiang, and M. Q. Weng, Phys. Rep. **493**, 61 (2010).

[3] M. A. Ruderman and C. Kittel, Phys. Rev. **96**, 99 (1954).

[4] T. Kasuya, Prog. Theor. Phys. **16**, 45 (1956); K. Yosida, Phys. Rev. **106**, 893 (1957).

[5] K. S. Novoselov, A. K. Geim, S. V. Morozov, D. Jiang, Y. Zhang, S. V. Dubonos, I. V. Grigorieva, and A. A. Firsov, Science **306**, 666 (2004).

[6] A. Bostwick, F. Speck, T. Seyller, K. Horn, M. Polini, R. Asgari, A. H. MacDonald, and E. Rotenberg, Science **328**, 999 (2010).

[7] Y. Barlas, T. Pereg-Barnea, M. Polini, R. Asgari, and A. H. MacDonald, Phys. Rev. Lett. **98**, 236601 (2007).

[8] M. Polini, R. Asgari, Y. Barlas, T. Pereg-Barnea, and A. H. MacDonald, Solid State Commun. **143**, 58 (2007).

[9] M. Polini, R. Asgari, G. Borghi, Y. Barlas, T. Pereg-Barnea, and A. H. MacDonald, Phys. Rev. B **77**, 081411(R) (2008); E. H. Hwang and S. Das Sarma, *ibid.* **77**, 081412 (2008); A. Qaiumzadeh and R. Asgari, New J. Phys. **11**, 095023 (2009).

[10] F. de Juan, A. G. Grushin, and M. A. H. Vozmediano, Phys. Rev. B **82**, 125409 (2010); P. E. Trevisanutto, C. Giorgetti, L. Reining, M. Ladisa, and V. Olevano, Phys. Rev. Lett. **101**, 226405 (2008); R. Roldán, M. P. López-Sancho, and F. Guinea, Phys. Rev. B **77**, 115410 (2008).

[11] R. Asgari, M. M. Vazifeh, M. R. Ramezanali, E. Davoudi, and B. Tanatar, Phys. Rev. B **77**, 125432 (2008).

[12] V. N. Kotov, B. Uchoa, V. M. Pereira, A. H. Castro Neto, and F. Guinea, Rev. Mod. Phys. **84**, 1067 (2012).

[13] A. Qaiumzadeh, Kh. Jahanbani, and R. Asgari, Phys. Rev. B **85**, 235428 (2012).

[14] M. A. H. Vozmediano, M. P. López-Sancho, T. Stauber, and F. Guinea, Phys. Rev. B **72**, 155121 (2005); D. A. Abanin, A. V. Shytov, and L. S. Levitov, Phys. Rev. Lett. **105**, 086802 (2010); A. M. Black-Schaffer, Phys. Rev. B **82**, 073409 (2010); M. Sherafati and S. Satpathy, *ibid.* **84**, 125416 (2011); A. Rao, M. W. B. Wilson, S. Albert-Seifried, R. Di Pietro, and R. H. Friend, *ibid.* **84**, 195411 (2012); H. Lee, E. R. Mucciolo, G. Bouzerar, and S. Kettemann, *ibid.* **86**, 205427 (2012); S. R. Power and M. S. Ferreira, *ibid.* **83**, 155432 (2011); P. Venezuela, R. B. Muniz, A. T. Costa, D. M. Edwards, S. R. Power, and M. S. Ferreira, *ibid.* **80**, 241413 (2009).

[15] S. Saremi, Phys. Rev. B **76**, 184430 (2007).

[16] M. Sherafati and S. Satpathy, Phys. Rev. B **83**, 165425 (2011); **84**, 125416 (2011).

[17] G. Bergmann, Phys. Rev. B **36**, 2469 (1987); A. Jagannathan, E. Abrahams, and M. J. Stephen, *ibid.* **37**, 436 (1988).

[18] G. Zarand and B. Janko, Phys. Rev. Lett. **89**, 047201 (2002).

[19] Q. Liu, C.-X. Liu, C. Xu, X.-L. Qi, and S.-C. Zhang, Phys. Rev. Lett. **102**, 156603 (2009).

[20] D. A. Abanin and D. A. Pesin, Phys. Rev. Lett **106**, 136802 (2011).

[21] M. Zareyan, H. Mohammadpour, and A. G. Moghaddam, Phys. Rev. B **78**, 193406 (2008); Y. Asano, T. Yoshida, Y. Tanaka, and A. A. Golubov, *ibid.* **78**, 014514 (2008); J. Linder, T. Yokoyama,

D. Huertas-Hernando, and A. Sudbø, Phys. Rev. Lett. **100**, 187004 (2008); A. G. Moghaddam and M. Zareyan, *ibid.* **105**, 146803 (2010); D. A. Abanin *et al.*, Science **332**, 328 (2011).

[22] A. Kalz, M. Arlego, D. Cabra, A. Honecker, and G. Rossini, Phys. Rev. B **85**, 104505 (2012); B. K. Clark, D. A. Abanin, and S. L. Sondhi, Phys. Rev. Lett. **107**, 087204 (2011); J. B. Fouet, P. Sindzingre, and C. Lhuillier, Eur. Phys. J. B **20**, 241 (2001).

[23] V. K. Dugaev, V. I. Litvinov, and J. Barnas, Phys. Rev. B **74**, 224438 (2006); B. Uchoa, V. N. Kotov, N. M. R. Peres, and A. H. Castro Neto, Phys. Rev. Lett. **101**, 026805 (2008).

[24] N. Tombros *et al.*, Nature (London) **448**, 571 (2007).

[25] N. M. R. Peres, F. Guinea, and A. H. Castro Neto, Phys. Rev. B **72**, 174406 (2005).

[26] Y.-W. Son, M. L. Cohen, and S. G. Louie, Nature (London) **444**, 347 (2006).

[27] G. W. Semenoff, Phys. Rev. Lett. **53**, 2449 (1984).

[28] L. M. Malard, J. Nilsson, D. C. Elias, J. C. Brant, F. Plentz, E. S. Alves, A. H. Castro Neto, and M. A. Pimenta, Phys. Rev. B **76**, 201401 (2007).

[29] Yu. S. Dedkov, M. Fonin, and C. Laubschat, Appl. Phys. Lett. **92**, 052506 (2008); L. V. Dzemiantsova, M. Karolak, F. Lofink, A. Kubetzka, B. Sachs, K. von Bergmann, S. Hankemeier, T. O. Wehling, R. Frömter, H. P. Oepen, A. I. Lichtenstein, and R. Wiesendanger, Phys. Rev. B **84**, 205431 (2011).

[30] S. Chesi and D. Loss, Phys. Rev. B **82**, 165303 (2010).

[31] H. Imamura, P. Bruno, and Y. Utsumi, Phys. Rev. B **69**, 121303(R) (2004).

[32] J. L. Fields, Math. Comp. **26**, 757 (1972).